Intrinsically irreversible light-driven engine

Stanley J. Watowich, Karl Heinz Hoffmann,[a] and R. Stephen Berry
Department of Chemistry and the James Franck Institute, The University of Chicago, Chicago, Illinois 60637

(Received 18 April 1985; accepted for publication 20 June 1985)

We examine a reciprocating heat engine which necessarily operates far from equilibrium and about an unstable steady state. The piston of the engine is driven by the nonlinear coupling of the working fluid to an external light source which provides high quality heat and to the environment into which waste heat is dumped. We determine the piston trajectories that optimize two different criteria of process performance, the maximization of work output, and the minimization of entropy production. The trajectories optimizing different performance goals are qualitatively different. In engines not dominated by friction losses, the cycle optimizing work output requires that the expansion stroke begins with a slight compression and the temperature of the working fluid increases briefly.

I. INTRODUCTION

Traditional equilibrium thermodynamics has long used ideal, reversible models to provide baseline values to judge the performance of real systems. Calculations based on reversible models provide rigorous bounds on the operation of real processes. These bounds often differ considerably from what can be obtained by even the best of processes that must operate in a finite time. Consequently, reversible models may suggest unrealistic bounds of performance, and mislead us into trying to accomplish unrealistic improvements.

To provide more realistic limits on the performance of real-time processes than those obtained from reversible models, time and rate constraints can be incorporated into the analysis of process performance. Several papers[1] have discussed systems in which loss mechanisms that couple the system to the environment are added to inherently reversible models. Only the main sources of dissipation or irreversibility are incorporated into these models. As such, these irreversible models represent broad classes of real-time processes and describe the dominant features of real systems. The generic models discussed in the above works are derived from the Carnot engine; irreversibilities all occur at boundaries between the environment and the reversible engine.

Recently, a new general class of thermodynamic engines has come under study. These engines have intrinsic irreversible losses inextricably linked to the driving forces for their operation. If operated reversibly these engines would not only yield no power, they would yield no work. A Carnot-based model is inappropriate to describe these systems that must exist in a state that is far from both equilibrium and steady-state conditions. Wheatley *et al.*[2] realized one such "dissipative heat engine" with their thermoacoustic engine. Ross and co-workers[3] proposed potentially oscillating chemical systems of N_2O_4 or $S_2O_6F_2$ and light. From these systems Mozurkewich and Berry[4] developed a theoretical model for a dissipative thermal engine driven by a reacting chemical system simultaneously coupled to an external light source which drives the engine and to the environment into which waste heat is dumped. They used this model to develop the piston path that optimizes the delivered power for such an engine.

In this paper, we extend the analysis of the intrinsically irreversible light-driven engine begun by Nitzan and Ross[3] and by Mozurkewich and Berry.[4] The goals of this analysis are a subset of the goals of finite-time thermodynamics:[5] (1) the determination of realistic process bounds (e.g., work output and entropy production) for this system, (2) the determination of the mode of operation that would yield these extremal bounds, and (3) the determination of the optimal path as a guide to improving the operation of real processes.

In Sec. II, we use an approximate step-heating function to model heat flow through a reaction chamber containing an exothermic reacting system. Friction losses, previously ignored, are explicitly included in our model. With such losses, process bounds are no longer independent of the cycle period and adiabatic strokes occurring in a short time compared to the cycle time can no longer be conveniently incorporated into the engine cycle. This current work goes beyond the prior investigations of both the Ross and Berry groups not only by the inclusion of more realistic constraints; more significant perhaps is that here we compare optimization for maximum power or work per cycle with optimization for minimum entropy production. These two are particularly important because, as Salamon and Nitzan have shown,[6] they determine the function whose maximum gives the economic optimum for operation of a thermodynamic system. The economically optimal solution can be written as a linear combination of the maximum power solution and the minimum entropy production solution, with linear coefficients that are the relative prices of the input factor costs and the output benefits.

Following the description of the model in Sec. II, we examine the operation of the idealized system under the hypothetical condition in which no account is taken for explicit extraction of work, to see whether there is a regime in which unstable, divergent oscillations of the engine's piston would occur. If such a regime exists, and we show that it does, then

[a] Present address: Institut für Theoret. Physik der Universität, Abt. Vielteilchen Physik, Philosophenweg 19, 6900 Heidelberg, Federal Republic of Germany.

 0021-8979/85/202893-09$02.40

a load can be matched to the engine to extract precisely enough work to maintain a regular reciprocal motion.

In Sec. III we optimize the time path for each of the two objectives of maximizing work per cycle and minimizing entropy production per cycle. In the language of optimal-control theory,[7] the form of calculus of variations employed here, the performance criteria are the objective functions. Their extrema are achieved by varying some control variable, in this case the time path of the piston. The optimal-control analysis provides a set of ordinary, coupled, nonlinear differential equations. Solving these equations yields the piston trajectory, and the time-parametrized forms of the state and process variables that optimize the desired performance criteria. Note that in this analysis the work load is implicitly balanced to stabilize the engine. This is the way virtually all idealized engine problems are treated; only in a few instances specifically concerned with inertial effects is this assumption set aside.[8]

Section IV discusses the trajectories and process bounds obtained for the two performance criteria. An interesting and suggestive operational difference between paths designed to maximize work output and paths designed to minimize entropy production is the reentrant behavior found in the former trajectories. This behavior was previously found in the optimal paths determined by Band and co-workers[9] and by Rubin.[10] If the compression ratio is fixed, the reentrant cycles in our study are transformed into four-stroke trajectories with isometric branches that allow the working fluid to heat or cool at the cycle's volume limits.

II. DESCRIPTION OF THE MODEL

Consider the dissipative light-driven engine shown in Fig. 1. A spatially homogeneous ideal gas is enclosed in a cylinder of cross section A_x. The cylinder is always in contact with an environment at constant temperature T_0 and constant pressure P_0. The engine is assumed to operate endoreversibly: the working fluid of the engine undergoes reversible transformations, limiting any irreversible processes to the boundary between the engine and the environment. The main loss mechanisms associated with operating the engine are heat conduction and piston friction. Conduction losses in this system arise from the flow of heat across a drop in temperature between the working fluid and the environment. We assume heat exchange obeys the Fourier expression

$$\frac{dQ_F}{dt} = -\kappa (T - T_0), \tag{1}$$

where T is the temperature of the working fluid and κ is the thermal conductance of the cylinder walls.

A piston of mass m exchanges work between the cylinder and a work reservoir in the environment, which we assume to be a high-inertia flywheel. We assume the piston is subject to frictional forces proportional to the piston's velocity.[11] The frictional work done on a well-lubricated sliding surface, W_f, in time t, is

$$W_f = \int_0^t \alpha \dot{x}^2 \, dt, \tag{2}$$

where $\dot{x}$ is the time rate of change of the displacement of the piston V and α is the coefficient of friction along the cylinder.

The working fluid is composed of species A and B, with the equilibrium

$$A \rightleftarrows B. \tag{I}$$

Additionally, species A enters into the following reaction: $A + \text{light} \rightarrow A^* \rightarrow A + \text{heat}$. Species A selectively absorbs incident light to form an excited species A^*. The excited species undergoes rapid thermal relaxation back to the ground state of A. Fluorescence is assumed to be negligible, so all the absorbed radiant energy is released as heat, which raises the temperature of the mixture confined in the cylinder. In a heat engine, the working fluid absorbs heat at a high temperature and rejects heat at a low temperature. This system is capable of producing work and operating as a heat engine when reaction (I) is exothermic.[4] When species A absorbs light and converts the light to heat, the temperature of the confined mixture rises, shifting the equilibrium to produce more A. In the present treatment the radiant energy contribution to heat flow through the system is modeled as a switching function,

$$\frac{dQ_R}{dt} = \beta \tan^{-1}\left[s\left(\frac{T - T_s}{T_s}\right)\right], \tag{3}$$

where β is the radiant energy flux or light intensity entering the system, T_s is the switching temperature, and s determines the steepness of the switch. The equilibrium of reaction (I) lies far to the right when $T < T_s$ and far to the left when $T > T_s$. In the limit $s \rightarrow \infty$ the radiant heat transfer function becomes a step function. If we set $T_s = T_0$ and $s = 10.0$, the net heat flow h given by the sum of Eqs. (1) and (3), reproduces the form of the net heating function for reactions where the higher enthalpy species selectively absorbs incident light. Examples of such reactions include NO_2 and SO_3F dimerization.

The dynamical equations governing the temperature, displacement, and velocity of the uncontrolled, dissipative light-driven engine are

$$\frac{dT}{dt} = \frac{-1}{NC_v}\left(\frac{NRTA_x \dot{x}}{V} - h\right), \tag{4a}$$

$$\frac{dV}{dt} = A_x \dot{x}, \tag{4b}$$

and

$$\frac{d\dot{x}}{dt} = \frac{1}{m}\left[A_x\left(\frac{NRT}{V} - P_0\right) - \alpha \dot{x}\right], \tag{4c}$$

respectively. The mole number N and the heat capacity C_v of the fluid are assumed constant.

Using the dimensionless variables $\xi = V/A_x x_0$, $\Theta = T/T_0$, $v = \dot{x} NC_v/\kappa x_0$ and $\tau = t\kappa/NC_v$ for displacement, tem-

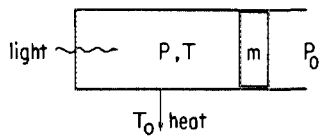

FIG. 1. Light-driven heat engine.

perature, velocity, and time, respectively, we rewrite Eqs. (4a)–(4c) as

$$\dot{\Theta} = \frac{-\beta_1 \Theta v}{\xi} + \beta_2 \tan^{-1}[s(\Theta - 1)] - \Theta + 1 , \quad (5a)$$

$$\dot{\xi} = v , \quad (5b)$$

and

$$\dot{v} = \beta_4 \Theta/\xi - \beta_5 - \beta_6 v . \quad (5c)$$

The dimensionless parameters are

$$\beta_1 = R/C_v, \quad \beta_2 = \beta/\kappa T_0,$$

$$\beta_4 = (NC_v)^2 NRT_0/\kappa^2 x_0^2 m ,$$

$$\beta_5 = A_x P_0 (NC_v)^2/\kappa^2 x_0 m ,$$

and

$$\beta_6 = \alpha NC_v/\kappa m .$$

Henceforth, the dot notation signifies the derivative $d(\ )/d\tau$.

Equations (5a)–(5c) give rise to three positive steady states when $s = 10.0$ and $0.1 < \beta_2 < 0.67975$. The middle steady state occurs at $\Theta = 1.0$. Mozurkewich and Berry[4] showed that this steady state corresponds to either an unstable node when $(\partial h/\partial T)_P > 0$ or an unstable focus when $(\partial h/\partial T)_S > 0$. The latter condition is necessary for a cyclic process to be capable of producing work. As shown in Ref. 12, the middle steady state is an unstable focus for the parameter sets used in this step-heated engine. The two other steady states are stable. For small displacements from the unstable steady state the piston oscillates to one of the bounding stable steady states.

III. OPTIMIZATION OF THE ENGINE

A. The engine

We now assume the piston is no longer free, but instead is attached to a controlling rod and motion transducer that can arbitrarily adjust the piston's velocity. For example, we could imagine a linkage connecting the piston to a tailored cam, which in turn connects to the high-inertia flywheel or work reservoir. An infinite number of cam shapes are possible, each generating its own time path for the piston. Our goal is to determine two particular piston paths: the path maximizing the work ouput of one cycle and the path minimizing the entropy production everywhere along a second cycle. The detailed description of the time path contains all the information about the evolution of the modeled process, including values for bounds on the process variables.

For simplicity, we decompose the continuous cycle of the irreversible light-driven engine into an expansion stroke and a compression stroke. The time spent on each stroke is fixed. Maximizing work output along each stroke simultaneously maximizes average power ouput along each stroke. Boundary conditions are determined by specifying the initial and final piston positions and the fluid temperatures at the beginning and end of each stroke. With the boundary conditions specified at each end of the time interval, constructing the optimal path along each stroke is equivalent to optimizing the entire cycle.

In the fixed time $t_f - t_i$ the net work output is

$$W = \int_{t_i}^{t_f} \left(\frac{NRTA_x \dot{x}}{V} - \alpha \dot{x}^2 \right) dt . \quad (6)$$

Irreversible entropy production during this time is

$$\Delta S = \int_{t_i}^{t_f} \left[-\kappa (T - T_0)\left(\frac{1}{T} - \frac{1}{T_0}\right) + \frac{\alpha \dot{x}^2}{T_0} \right] dt . \quad (7)$$

Rewriting Eqs. (6) and (7) in the dimensionless variables introduced earlier gives

$$\Gamma = \int_{\tau_i}^{\tau_f} \left(\frac{\Theta v}{\xi} - \beta_3 v^2 \right) d\tau , \quad (8)$$

and

$$\Sigma = \int_{\tau_i}^{\tau_f} \left[-(\Theta - 1)\left(\frac{1}{\Theta} - 1\right) + \beta_1 \beta_3 v^2 \right] d\tau , \quad (9)$$

respectively, where $\Gamma = W/\beta_0$, $\Sigma = \beta_1 T_0 \Delta S/\beta_0$, $\beta_0 = NRT_0$, and $\beta_3 = \beta_6/\beta_4$.

The state variables, Θ and ξ are subject to the differential constraints given by Eqs. (5a) and (5b), respectively. Boundary conditions specifying the expansion stroke are

$$\Theta(\tau_0) = \Theta_i , \quad (10a)$$

$$\Theta(\tau_1) = \Theta_f , \quad (10b)$$

$$\xi(\tau_0) = \xi_i , \quad (10c)$$

and

$$\xi(\tau_1) = \xi_f . \quad (10d)$$

Boundary conditions for the compression stroke are

$$\Theta(\tau_1) = \Theta_f , \quad (11a)$$

$$\Theta(\tau_2) = \Theta_i , \quad (11b)$$

$$\xi(\tau_1) = \xi_f , \quad (11c)$$

and

$$\xi(\tau_2) = \xi_i . \quad (11d)$$

A Hamiltonian is constructed for each of the objective functions given by Eqs. (6) and (7). The control variable $v(\tau)$ that maximizes the Hamiltonian simultaneously maximizes the objective function. The control variable is given as a function of state variables $\Theta(\tau)$ and $\xi(\tau)$, and their respective Lagrange multipliers $\lambda_1(\tau)$ and $\lambda_2(\tau)$. Along the extremal path the control variable v necessarily satisfies the differential constraints provided by optimal-control theory for the state variables and the Lagrange multipliers.

B. Cycle of maximum work

Consider the problem of maximizing work output as given by Eq. (8). The Hamiltonian for this problem is

$$H_\Gamma = \Theta v/\xi - \beta_3 v^2 + \lambda_1 \{ -\beta_1 \Theta v/\xi + \beta_2 \tan^{-1}[s(\Theta - 1)] - \Theta + 1 \} + \lambda_2 v .$$

The time evolution of λ_1 and λ_2, the canonical equations conjugate to Eqs. (5a) and (5b), respectively, is

$$\dot{\lambda}_1 = -\frac{\partial H_\Gamma}{\partial \Theta} = \lambda_1 \left(\frac{\beta_1 v}{\xi} - \frac{\beta_2}{\{[s(\Theta - 1)]^2 + 1\}/s} + 1 \right) - \frac{v}{\xi} \quad (12a)$$

and

$$\dot{\lambda}_2 = -\frac{\partial H_\Gamma}{\partial \xi} = \frac{\Theta v}{\xi^2}(1-\beta_1\lambda_1)\,. \tag{12b}$$

For an unconstrained control variable the optimal-piston trajectory necessarily satisfies the condition

$$\frac{\partial H}{\partial v} = 0\,,$$

which for H_Γ yields

$$v = (-1/2\beta_3\xi)(\beta_1\lambda_1\theta - \lambda_2\xi - \Theta)\,. \tag{13}$$

C. Cycle of minimum entropy production

We now turn to the problem of minimizing the entropy production as expressed by Eq. (9). The Hamiltonian for this system is

$$H_\Sigma = (\Theta-1)(1/\Theta-1) - \beta_1\beta_3 v^2 + \lambda_1\{-\beta_1\Theta v/\xi + \beta_2\tan^{-1}[s(\Theta-1)] - \Theta + 1\} + \lambda_2 v\,.$$

The equations describing the time evolution of λ_1 and λ_2 are

$$\dot{\lambda}_1 = -\frac{\partial H_\Sigma}{\partial\Theta} = \lambda_1\left(\frac{\beta_1 v}{\xi} - \frac{\beta_2}{\{[s(\Theta-1)]^2+1\}/s} + 1\right) + 1 - \frac{1}{\Theta^2}\,, \tag{14a}$$

and

$$\dot{\lambda}_2 = -\frac{\partial H_\Sigma}{\partial\xi} = \frac{-\beta_1\lambda_1\Theta v}{\xi^2}\,. \tag{14b}$$

The optimal piston trajectory is

$$v = (-1/2\beta_1\beta_3\xi)(\beta_1\lambda_1\Theta - \lambda_2\xi)\,. \tag{15}$$

The path optimizing the objective function along each stroke is given by the system of nonlinear differential equations for Θ, ξ, λ_1, and λ_2, subject to the constraints imposed by the control variable and the boundary conditions. This system of equations is solved numerically using an initial-value differential equation solver. A shooting method is used to satisfy the mixed boundary conditions. Initial values for $\lambda_1(\tau_0)$ and $\lambda_2(\tau_0)$ are chosen from a range of values supplied by a linear stability analysis of the optimal system.[12] The differential equations are integrated and the resulting values of $\Theta(\tau_f)$ and $\xi(\tau_f)$ are compared with the desired boundary conditions at the end points. The initial values used for $\lambda_1(\tau_0)$ and $\lambda_2(\tau_0)$ are modified by a multivariate function optimizing routine, VMCON,[13] to minimize the difference between the desired and resultant values of $\Theta(\tau_f)$ and $\xi(\tau_f)$.

TABLE I. Engine parameters.

Stroke times	
expansion stroke $(\tau_1-\tau_0)$	1.0
compression stroke $(\tau_2-\tau_1)$	1.0
End temperatures	
Θ_i	1.1
Θ_f	0.9
End positions	
ξ_i	1.0
ξ_f	2.0
Radiant heat flow	
steepness of heating switch (s)	10.0
β parameters	
β_1	0.4
β_2	0.65
β_3	0.01

TABLE II. Variations from the standard case engine.

Case	β_1	β_2	β_3
Std	0.4	0.65	0.01
I	0.4	0.55	0.01
II	0.4	0.45	0.01
III	0.4	0.35	0.01
IV	0.4	0.2755	0.01
V	0.4	0.65	0.025
VI	0.4	0.65	0.05
VII	0.4	0.65	0.10
VIII	0.4	0.65	0.15
IX	0.4	0.65	0.20

IV. RESULTS

Piston trajectories yielding either maximum work output or minimum entropy production (hence termed the optimal work path and the optimal entropy production path, respectively) were calculated for the dissipative light-driven engine. Optimal paths were determined for several β_2 and β_3 values; these values depend on the mechanical construction of the engine. The fluid temperature and the piston displacment are fixed at the end points of each stroke to specify uniquely the state of the confined gas at the beginning and end of each stroke. Fluid temperatures at the end points of each stroke were chosen such that $\Theta_{l,ss} < \Theta_f < \Theta_{us} < \Theta_i < \Theta_{h,ss}$, where $\Theta_{l,ss}$ refers to the lower temperature stable steady state, $\Theta_{h,ss}$ refers to the higher temperature stable steady state, and Θ_{us} refers to the temperature of the unstable steady state of Eqs. (5a)–(5c).

Table I contains the parameter values used for the standard reference engine. Variations in β_2 and β_3 from the standard case engine are listed in Table II. Table III lists energies and entropies found for the optimal work path over a complete cycle. Net work output Γ_{net} is the work output integral, Eq. (8), evaluated for the expansion and compression strokes. The dimensionless total friction loss per cycle is

TABLE III. Net process values for maximum work output.

Case	Γ_{net}	Λ_F	Λ_Q	Σ_{net}	Σ_F	Σ_Q
Std	0.2392	0.2027	0.6195	0.1921	0.08108	0.1110
I	0.1636	0.1431	0.4375	0.1349	0.05724	0.07766
II	0.1010	0.09210	0.2833	0.08884	0.03684	0.05200
III	0.05254	0.05156	0.1676	0.05439	0.02062	0.03377
IV	0.01808	0.04015	0.09083	0.03983	0.01606	0.02377
V	0.06699	0.1760	0.1485	0.1049	0.07040	0.03450
VI	−0.06335	0.2002	0.03543	0.09364	0.08006	0.01358
VII	−0.2286	0.3054	0.01326	0.1289	0.1222	0.006728
VIII	−0.3791	0.4478	0.01159	0.1851	0.1791	0.005988
IX	-	-	-	-	-	-

TABLE IV. Net process values for minimum entropy production.

Case	Γ_{net}	Λ_F	Λ_Q	Σ_{net}	Σ_F	Σ_Q
Std	0.01307	0.03085	0.006690	0.01607	0.01234	0.003730
I	0.01354	0.02739	0.008405	0.01522	0.01096	0.004264
II	0.01243	0.02497	0.01141	0.01506	0.009988	0.005072
III	0.008817	0.02544	0.01874	0.01688	0.01018	0.006704
IV	-	-	-	-	-	-
V	−0.02368	0.07453	0.008083	0.03416	0.02981	0.004378
VI	−0.09366	0.1479	0.008760	0.06382	0.05916	0.004656
VII	−0.2388	0.2959	0.009170	0.1229	0.1183	0.004556
VIII	−0.3854	0.4425	0.009318	0.1819	0.1770	0.004916
IX	−0.5324	0.5899	0.009395	0.2409	0.2359	0.004960

$$\Lambda_F = \beta_3 \int_{\text{cycle}} v^2 \, d\tau .$$

The dimensionless total heat leak per cycle is

$$\Lambda_Q = \beta_1^{-1} \int_{\text{cycle}} (\Theta - 1) \, d\tau .$$

Entropy production for the complete cycle is Σ_{net}, defined by Eq. (9). Entropy production from friction and heat leak are given as

$$\Sigma_F = \beta_1 \beta_3 \int_{\text{cycle}} v^2 \, d\tau ,$$

and

$$\Sigma_Q = \int_{\text{cycle}} (1 - \Theta) \left(\frac{1}{\Theta} - 1 \right) d\tau ,$$

respectively. Table IV lists identical process information for the optimal entropy production path.

As expected, work ouput and entropy production are greater along cycles constructed to maximize work output than along cycles designed to minimize entropy production. If the dimensionless friction coefficient has a high enough value, the net work output along the optimal path is negative.

In Table V we tabulate the efficiency of the optimized engine. Efficiency is defined as $\eta_{net} = W_{net}/Q_R$. Net work output for the dissipative system is $W_{net} = \beta_0 \Gamma_{net}$. Radiant heat input to the system is calculated as

TABLE V. Efficiency of optimized engines. $[\Omega_R = \int_{cycle} \beta_2 \tan^{-1}[s(\Theta - 1)] \, d\tau$ when $\Theta \geq 1.0$; $\eta_{net} = \beta_1 \Gamma_{net}/\Omega_R .]$

	Maximum work ouput		Minimum entropy production	
Case	Ω_R	η_{net}	Ω_R	η_{net}
Std	0.8704	0.1099	0.2149	0.02432
I	0.6775	0.09660	0.2013	0.02690
II	0.4984	0.08108	0.1862	0.02670
III	0.3382	0.06216	0.1733	0.02035
IV	0.2371	0.03050	-	-
V	0.5559	0.04820	0.2347	−0.04036
VI	0.4096	−0.06188	0.2442	−0.1534
VII	0.3025	−0.3023	0.2499	−0.3822
VIII	0.2829	−0.5360	0.2520	−0.6116
IX	-	-	0.2531	−0.8416

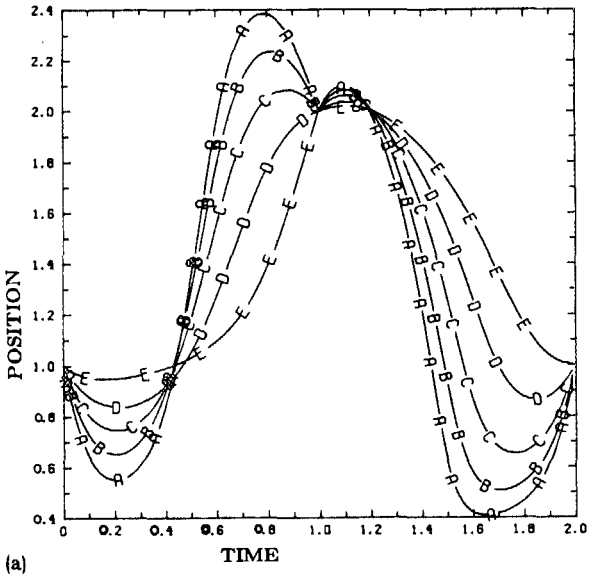

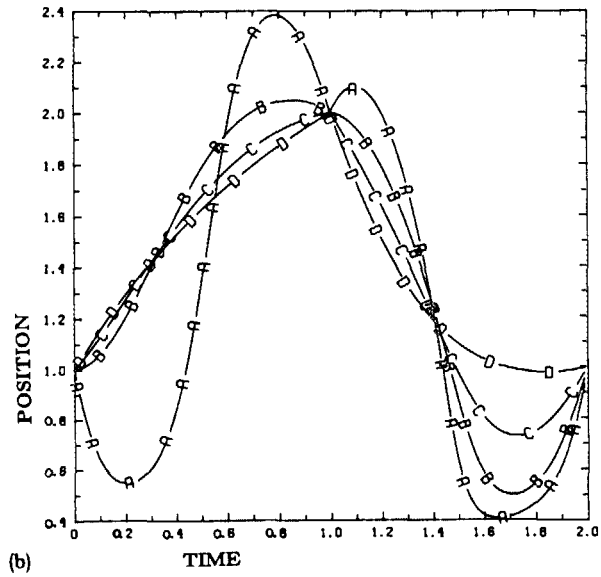

FIG. 2. (a) Piston position profiles for maximum work output. Curve assignments: Standard case (A), case I (B), case II (C), case III (D) and case IV (E). These, and all following curves, were calculated using approximately 300 points. (b) Piston position profiles for maximum work output. Curve assignments: Standard case (A), case V (B), case VI (C), and case VIII (D).

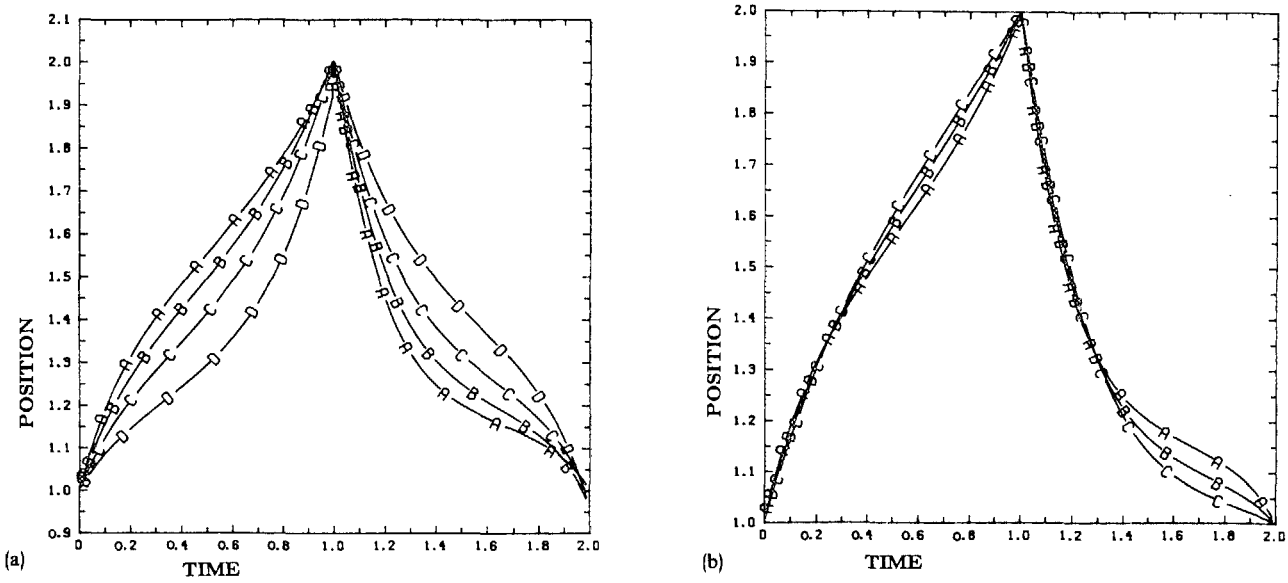

FIG. 3. (a) Piston position profiles for minimum entropy production. Curve assignments: Standard case (A), case I (B), case II (C), and case III (D). (b) Piston position profiles for minimum entropy production. Curve assignments: Standard case (A), case V (B), and case VIII (C).

$$Q_R = \frac{\beta_0}{\beta_1}\Omega_R = \frac{\beta_0}{\beta_1}\int_{\text{cycle}} q_R \, d\tau , \tag{16}$$

where

$$q_R = \beta_2 \tan^{-1}[s(\Theta - 1)], \quad \text{when } \Theta \geqslant 1.0 ,$$
$$= 0, \quad \text{when } \Theta < 1.0 .$$

The efficiency of an engine is greater along a path that maximizes work output than along a path that minimizes entropy production. We conjecture, but do not prove, that this is a general feature of dissipative engines.

Figures 2 and 3 show the piston trajectories $\xi(\tau)$ for the respective extrema of maximum work output and minimum entropy production. Figures 4 and 5 plot the temperature profiles $\theta(\tau)$ corresponding to maximum work output and minimum entropy production, respectively. The paths optimizing work ouput with low-friction coefficient show the working fluid being compressed at the beginning of the expansion stroke and expanded at the beginning of the compression stroke. In the majority of these cases the piston also tends to overshoot the fixed end point. The reentrant behavior exhibited along the optimal work path is similar to cycle paths produced by Band and co-workers.[9] To produce maximum work output the piston moves to increase its internal pressure along the expansion stroke and to decrease its internal pressure along the compression stroke. The increased

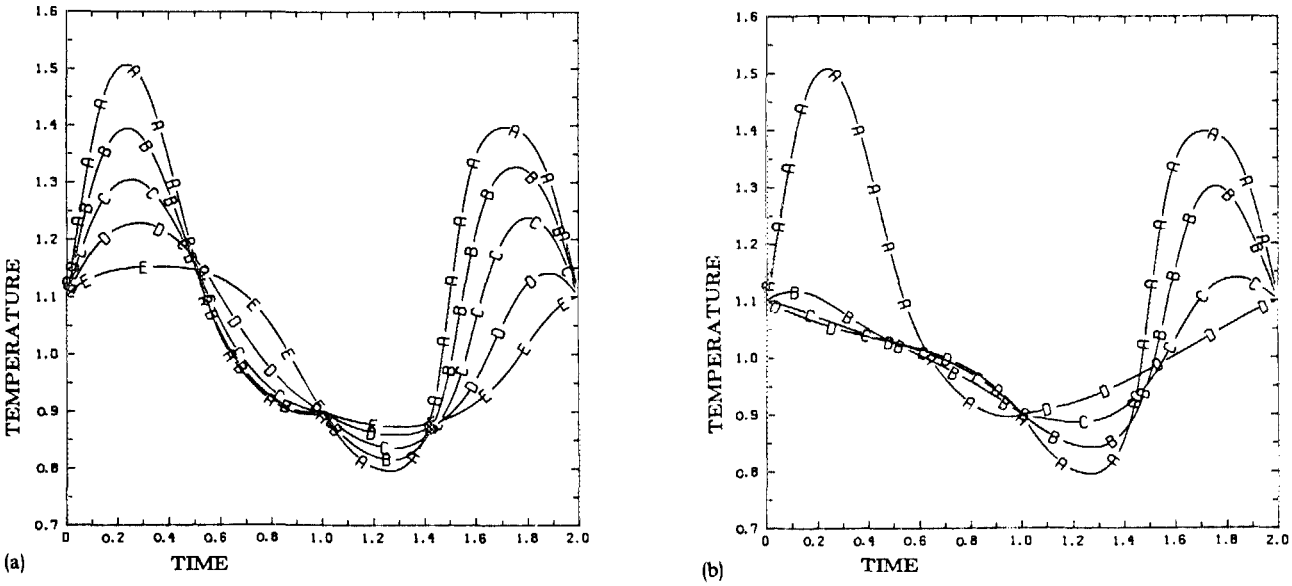

FIG. 4. (a) Internal temperature profiles for maximum work output. Curve assignments: Standard case (A), case I (B), case II (C), case III (D), and case IV (E). (b) Internal temperature profiles for maximum work output. Curve assignments: Standard case (A), case V (B), case VI (C), and case VII (D).

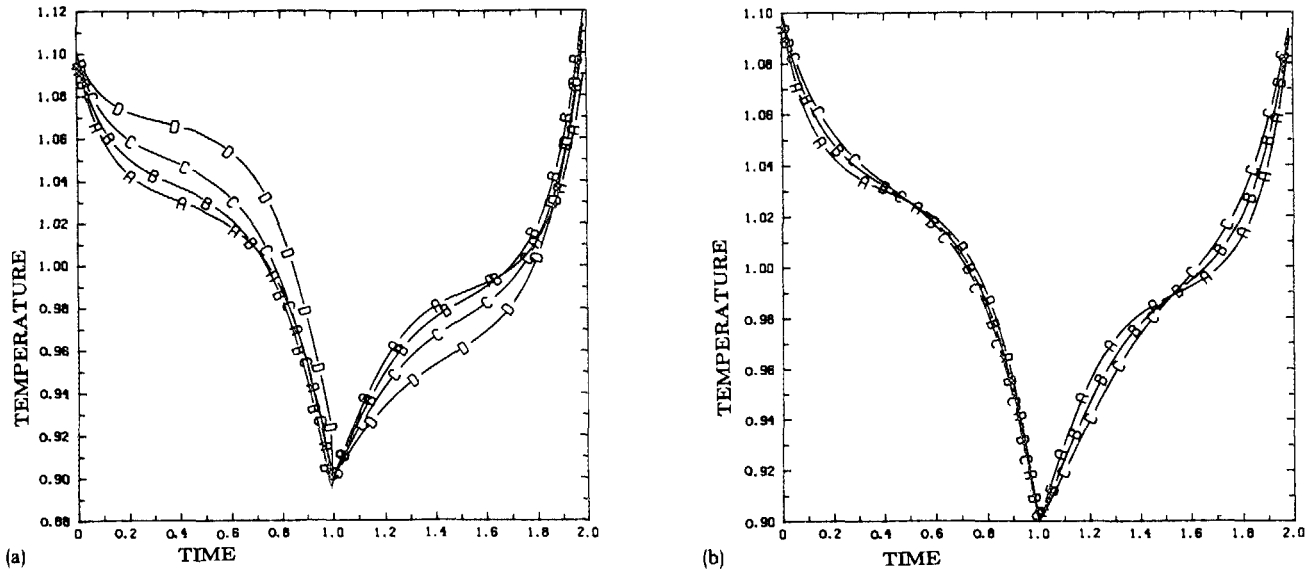

FIG. 5. (a) Internal temperature profiles for minimum entropy production. Curve assignments: Standard case (A), case I (B), case II (C), and case III (D). (b) Internal temperature profiles for minimum entropy production. Curve assignments: Standard case (A), case V (B), and case VIII (C).

TABLE VI. Net Process values for maximum work output.

Case	Γ_{net}	Λ_F	Λ_Q	Σ_{net}	Σ_F	Σ_Q	η_{net}
IV (fixed compression ratio)	0.01714	0.03859	0.07105	0.03705	0.01544	0.02161	0.03012

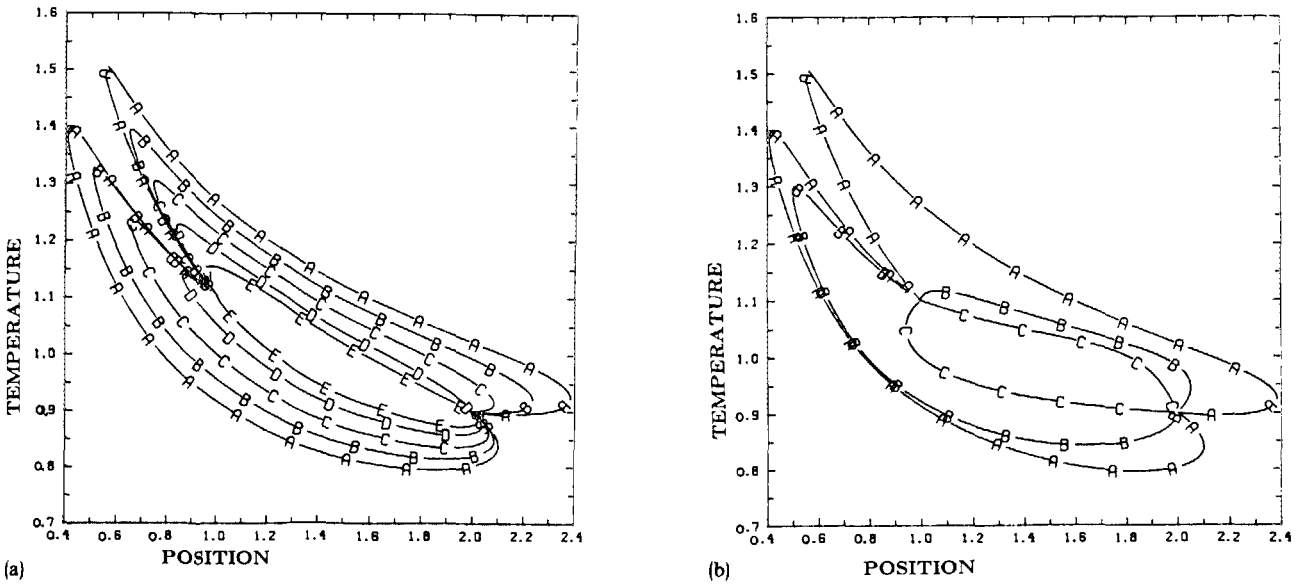

FIG. 6. (a) Time-parametrized curves of temperature vs position for maximum work output. Curve assignments: Standard case (A), case I (B), case II (C), case III (D), and case IV (E). (b) Time-parametrized curves of temperature vs position for maximum work output. Curve assignments: Standard case (A), case V (B), and case VII (C).

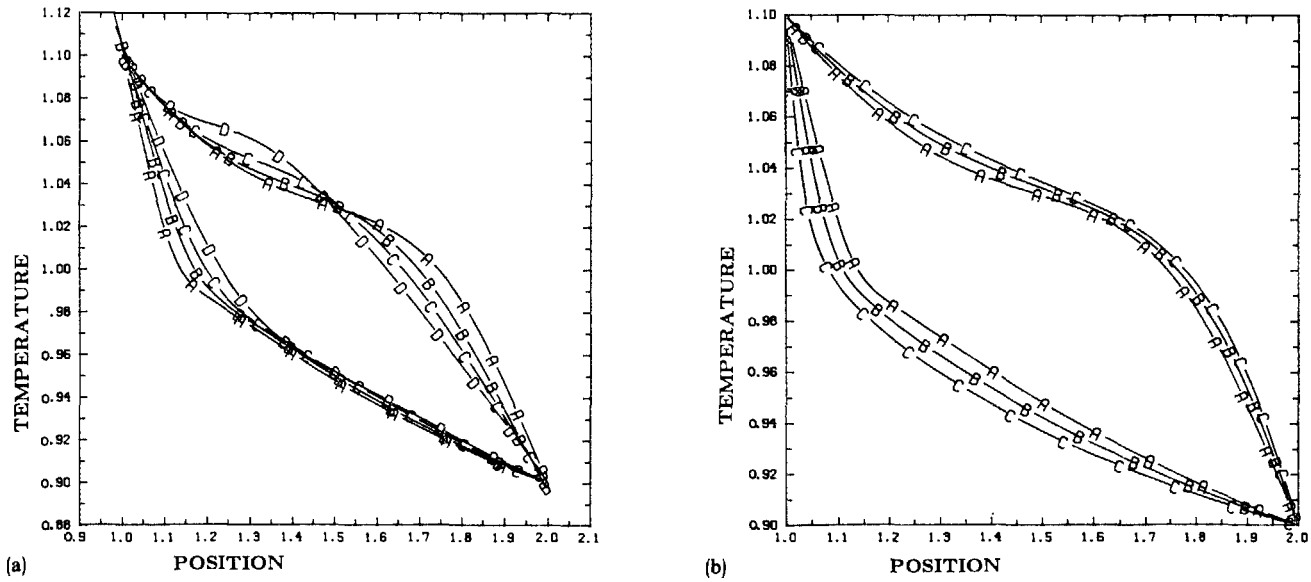

FIG. 7. (a) Time-parametrized curves of temperature vs position for minimum entropy production. Curve assignments: Standard case (A), case I (B), case II (C), and case III (D). (b) Time-parametrized curves of temperature vs position for minimum entropy production. Curve assignments: Standard case (A), case V (B), and case IX (C).

piston velocity results in increased friction losses, while the increased temperature results in greater heat leak losses. The increase in pressure-volume (P-V) work more than compensates for losses along the reentrant positions of the cycle, thus providing greater net work output. Results of calculations done for an engine with a compression ratio ξ_f/ξ_i fixed by selected points i and f are presented in Table VI.

Figures 6 and 7 plot the time-parametrized curves of temperature against position for cycles designed to maximize work output and minimize entropy production, respectively. The cycles maximizing work output exhibit a "nesting" order, whereby the optimal path for one engine is completely enveloped within the optimal path of a second engine. In plots of temperature versus position, nesting behavior is observed in optimal work paths for progressive changes in a single parameter.

Figure 8 compares the pressure-volume plots for the optimal cycles of the standard engine. The cycle maximizing work output completely envelopes the minimum entropy production cycle. This behavior is observed in all engines listed in Table II. From this limited number of observations we suggest that such "nesting" of the pressure-volume curves of the minimum entropy trajectory inside the maximum work trajectory is a general feature of this type of dissi-

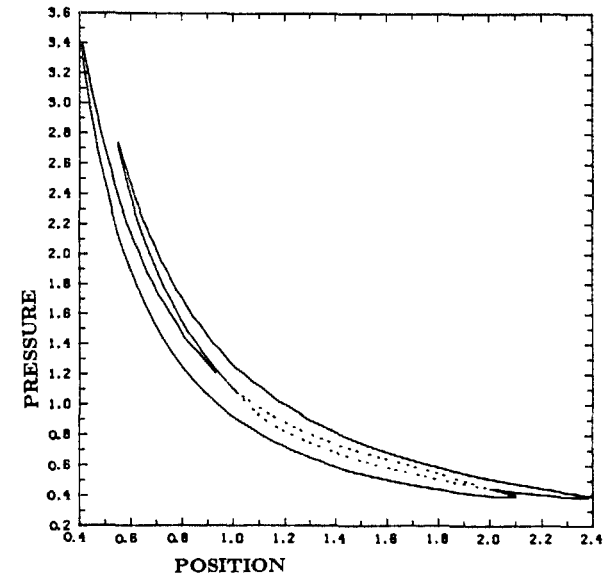

FIG. 8. Time-parametrized curves of pressure vs position for standard case engine. Curve assignments: optimal work path (solid line), optimal entropy production path (dotted line).

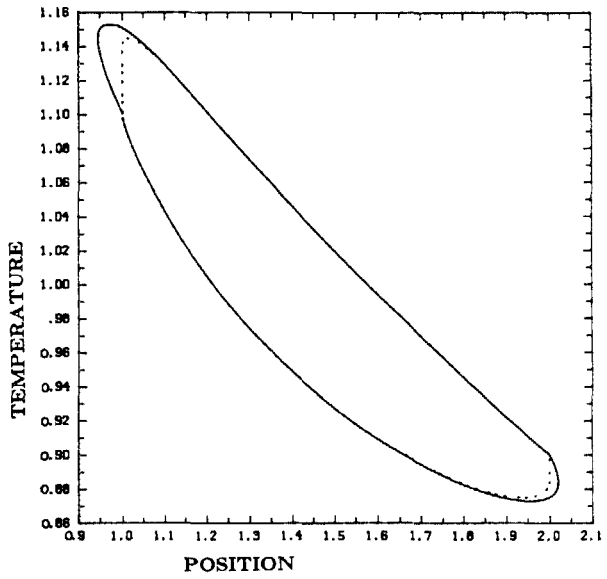

FIG. 9. Time-parametrized curves of temperature vs position for case IV engine. Curve assignments: uncontrained piston position (solid line), fixed compression ratio (dotted line).

pative engine. The time-parametrized curve of P-V work for maximum work output always lies above the time-parametrized curve of P-V work for minimum entropy production.

Figure 9 reveals the effect of fixed compression ratio on the time-parametrized temperature-position plots for a representative engine. Between the position endpoints imposed by the fixed compression ratio, the optimal trajectory for the engine with a fixed compression ratio is nearly identical to the optimal trajectory for the engine with an unconstrained compression ratio. The optimal volume-constrained system is a four-stroke engine, with isometric branches connecting branches of maximum work output. Similar branches were found by Rubin[10] in a Carnot-based endoreversible model with only heat conduction losses. In Rubin's system, maximizing average power output gave an eight-branch cycle, including two fixed volume branches.

V. DISCUSSION AND SUMMARY

To function as a work-producing engine the light-driven dissipative system must necessarily operate far from equilibrium and in finite time. Performance bounds determined by equilibrium thermodynamics are not applicable to this system since the infinitely slow limit of our dissipative system is not reversible. Lacking a reversible bound, we have investigated the behavior of the light-driven engine at the extrema of maximum work output and minimum entropy production. This analysis provides bounds on the operation of the engine, bounds that are more realistic than reversible limits in equilibrium thermodynamics since the major sources of irreversibility are incorporated into our model. In addition, this analysis provides insights into the relative importance of the system's rate parameters and boundary conditions in determining performance limits and optimal-operating behavior. The paths optimizing the performance criteria balance heat conduction losses against friction losses. The optimal work path further balances the conflicting aims of increasing the P-V work by increasing the compression ratio and the temperature of the working fluid against reducing friction and heat conduction losses by lowering compression ratios and working fluid temperature. Along the optimal work path, heat conduction losses are nearly three times as large as friction losses for low friction coefficients. At progressively larger values of the friction coefficient, losses from friction increasingly dominate losses from heat conduction.

Similar behavior is observed in engines operating to minimize entropy production. At larger values of the heat conduction parameter (smaller β_2 values) entropy production due to heat conduction approaches entropy production due to friction. This implies that friction is the dominant loss influencing the piston path for the parameter values studied. For the minimum entropy case with these parameters, the above observations indicate that reducing friction losses offer the greatest potential for improving the optimal performance, that is, for reducing the minimum amount of entropy produced in this system.

The importance of the parameter values describing the loss terms depends on which performance criterion is optimized. Net entropy production along the cycle minimizing this quantity is influenced strongly by only β_3. Net entropy production changes slightly and in a nonmonotonic manner for variations in β_2. The form of the optimal-entropy production cycle remains invariant for changes in β_2 and β_3.

In contrast, the optimal-work trajectory and the net work output along the optimal trajectory respond strongly to variations in the β_2 and β_3 parameters. The reentrant behavior of the optimal-work cycles indicate design strategies for real dissipative engines operating with finite rate constraints and in finite time. The optimal trajectories suggest that for engines with friction losses less than heat conduction losses, net work output can be increased by the compression ratio and the temperature of the working fluid. The construction of optimal paths for models that incorporate only the major process losses provides a method for determining to a first approximation the compression ratio that provide maximum net work output. For engines with a piston path bounded by the volume at the end points of each stroke, the optimal work path suggests the two-stroke cycle should be replaced by a four-stroke cycle composed of two constant-volume branches connecting two maximum work branches.

This model calculation is a means to see the behavior of the dissipative with some of the complexities of real reactive working fluids simplified, particularly by use of the step-heating model. A more realistic analysis follows, which is intended as a basis for design of a physical test of such an engine.

ACKNOWLEDGMENT

This research was supported by Contract DE-ACO2-80ER10646 of the U. S. Department of Energy.

[1] B. Andresen, P. Salamon, and R. S. Berry, J. Chem. Phys. **66**, 1571 (1977); B. Andresen, R. S. Berry, A. Nitzan, and P. Salamon, Phys. Rev. A **15**, 2086 (1977); D. Gutkowicz-Krusin, I. Procaccia, and J. Ross, J. Chem. Phys. **69**, 3898 (1978); M. H. Rubin, Phys. Rev. A **22**, 1741 (1980); M. Mozurkewich and R. S. Berry, J. Appl. Phys. **54**, 3651 (1983).
[2] J. Wheatley, T. Hofler, G. W. Swift, and A. Migliori, Phys. Rev. Lett. **50**, 499 (1983).
[3] A. Nitzan and J. Ross, J. Chem. Phys. **59**, 241 (1973); E. C. Zimmermann and J. Ross, J. Chem. Phys. **80**, 720 (1984).
[4] M. Mozurkewich and R. S. Berry, J. Appl. Phys. **54**, 3651 (1983).
[5] B. Andresen, R. S. Berry, M. J. Ondrechen, and P. Salamon, Acct. Chem. Res. **17**, 266 (1984).
[6] P. Salamon and A. Nitzan, J. Chem. Phys. **74**, 3546 (1981).
[7] P. Naslin, *Essentials of Optimal Control* (Boston Technical, Cambridge, MA, 1969); A. E. Bryson and Y. C. Ho, *Applied Optimal Control* (Wiley, New York, 1975).
[8] V. Fairén and J. Ross, J. Chem. Phys. **75**, 5485, 5490 (1981).
[9] Y. H. Band, O. Kafri, and P. Salamon, Chem. Phys. Lett. **72**, 127 (1980).
[10] M. H. Rubin, Phys. Rev. A **22**, 1741 (1980).
[11] C. F. Taylor, *The Internal Combustion Engine in Theory and Practice* (MIT, Cambridge, MA, 1966), Vol. 1, pp. 312–355.
[12] S. Watowich, J. Krause, and R. S. Berry, in *Applications of Computer Algebra*, edited by R. Pavelle (Kluwer Academic, Hingham, MA, 1985).
[13] R. L. Crane, K. E. Hillstrom, and M. Minkoff, *Solution of the General Nonlinear Programming Problem with the Subroutine VMCON* (ANL-80-64, Argonne National Laboratory, Argonne, IL).